COMMON CHARACTERISTICS OF PROVEN SEALING AND LEAKING FAULTS

S.J. Naruk[1], W.F. Dula[1], J.P. Busch[1], B.A. Couzens-Schultz[1], L. Garmezy[1], H. Griffiths[2], A.M. Gunst[1], C.A. Hedlund[2], E. McAllister[1], U.O. Onyeagoro[1], B.M. Ozumba[3], A.Younes[1]
[1]Shell International Exploration and Production, Inc., [2]Shell Deepwater Services, Inc., [3]Shell Petroleum Development Co.

Faults in general may seal as a result of a very wide variety of processes, including juxtaposition, gouges, clay smears, cementation, grain-size reduction and/or diagenesis. The relative significance of each mechanism is commonly interpreted on the basis of theoretical fault models, outcrop studies, or limited field studies. In relatively shale-rich stratigraphic sections, sand-on-shale juxtaposition is commonly interpreted to be the primary factor determining whether or not a fault seals (e.g., Allan, 1989). Sealing sand-on-sand fault contacts also occur, however. In relatively shale-rich sections, this sealing capacity is thought to be a function of clay smear potential (CSP)(e.g., Bouvier et al., 1989; Jev et al., 1993) or shale gouge ratio (SGR) (e.g., Yielding et al., 1997, 1999). Sealing sand-on-sand fault contacts also occur in reservoir sections that are essentially devoid of shale or clay, however, and in these cases the fault seal capacity is attributed to some combination of orientation, total depth and throw (e.g., Knott, 1993), or more specifically the conditions of faulting and the amount of self-healing experienced by the fault rock (e.g., Hippler, 1997; Knipe et al., 1997).

This paper discusses results of studies of faults which are known to seal or leak based on sub-surface data from ~30 well-constrained fields in 8 basins (Figure 1). Sealing faults were identified from proven differences in fluid levels, compositions, or gradients across seismically visible faults. Non-sealing faults were interpreted to occur where the fluid levels, compositions and gradients were all the same across the faults. Well and 3D seismic data were used to define both the structural and stratigraphic architecture of the fields, and to make fault plane juxtaposition diagrams of each sealing or non-sealing fault. Each fault was gridded and contoured for both SGR (shale gouge ratio) and CSP (clay smear potential), and the results were compared to the demonstrable pressure differences (or the absence of them) across the fault.

The most salient conclusion is that juxtaposition is not the most significant factor distinguishing sealing from leaking faults. Sealing sand-on-sand (and sandstone-on-sandstone) fault contacts are common in every major play studied (Figures 2 - 4). Conversely, leaking sand-on-shale contacts, although more difficult to conclusively document, have been identified as well. Furthermore, faults which appear to have been non-sealing prior to production, are commonly observed to act as very strong baffles during production, with thousands of psi pressure difference occurring across the faults (Figure 5).

In most plays having stratigraphic sections with sand/shale (net/gross) ratios less than about 80%, the composition of the fault zone is the primary factor controlling the faults' seal capacities. Faults from many different basins show a common first-order correlation of fault seal capacity with fault zone composition regardless of in situ stress, burial depth and burial history, and clay type.

In some cases, both SGR and CSP correlate positively with fault seal capacity (e.g., Figure 6). In other cases, only one parameter correlates with fault seal capacity. In still other cases, there is simply insufficient shale or clay in the faulted section for either CSP or SGR to explain the observed seals.

The difference between CSP and SGR is explicable in that the two algorithms represent significantly different physical processes. The Shale Gouge Ratio calculates the percent of shale dragged past

each point on a fault plane. It assumes the fault creates a homogeneous gouge with a composition equal to the average composition of the wall rocks that have slipped past the fault, regardless of the actual fault deformation processes. In contrast, Clay Smear Potential (CSP) calculates the length of a continuous shale tail smeared out in the fault zone. It assumes that the normal stress across the fault is less than the vertical load on the shale beds, and that if the shale is fluid enough, and the fault moves slowly enough, shale will be squeezed from the sub-horizontal beds into the fault zone
Cross plots of SGR and CSP as functions of each other demonstrate that they are not related in any simple or obvious way. Along a single fault, any given value of CSP has multiple corresponding values of SGR (Figure 7).

The common occurrence of demonstrably sealing sand-on-sand fault contacts, as well as the occurrence of demonstrably leaking sand-on-shale fault contacts, indicate that juxtaposition is not a primary control on fault seal capacity. Global comparisons of known sealing and leaking faults show positive linear correlations between the retained pressures, and the gouge compositions as described by SGR algorithms in some cases, and the gouge compositions as described by CSP algorithms in other cases. Where the net/gross of the faulted section is greater than ~20%, sealing sand-on-sand fault contacts are still common, but the retained pressures show no correlation with either SGR or CSP algorithms.

References

Allan, U.S., 1989, Model for hydrocarbon migration and entrapment within faulted structures: AAPG Bulletin, v. 73, p. 803-811.

Bouvier, J.D., C.H. Kaars-Sijpesteijn, D.F. Kluesner, C.C. Onyejekwe, ad R.C. van der pal, 1989, Three-dimensional seismic interpretation and fault sealing investigations, Nun River Field, Nigeria: AAPG Bulletin, v. 73, p. 1397-1414.

Hippler, S.J., 1997, Microstructures and diagenesis in North Sea fault zones: Implications for fault seal potential and fault migration rates, in R.C. Surdam, ed., Seals, traps, and the petroleum system: AAPG Memoir 67, p.85-101.

Jev, B.I., C.H. Kaars-Sijpesteijn, M.P.A.M. Peters, N.L. Watts, and J.T. Wilkie, 1993, Akaso Field, Nigeria: Use of integrated 3-D seismic, fault slicing, clay smearing and RFT pressure data on fault trapping and dynamic leakage, AAPG Bulletin, v. 77, p. 1389-1404

Knipe, R.J., Q.J. Fisher, G. Jones, M.R. Clennell, A.B. Farmer, A. Harrison, B. Kidd, E. McAllister, J.R. Porter, and E.A. White, 1997, Fault seal analysis: successful methodologies, application and future directions, in P. Moller-Pedersen and A.G. Koestler, eds., Hydrocarbon seals: Importance for exploration and production: NPF special publication 7, p. 15-40.

Knott, S.D., 1993, Fault seal analysis in the North Sea: AAPG Bulletin, v. 77, p. 778-792.

Yielding, G., B. Freeman, and D.T. Needham, 1997, Quantitative fault seal prediction: AAPG Bulletin, v. 81, p. 987-917

Yielding, G., J.A. Overland and G. Byberg, 1999, Characterization of fault zones for reservoir modeling: An example from the Gullfaks Field, Northern North Sea: AAPG Bulletin, v. 83, p.925-951.

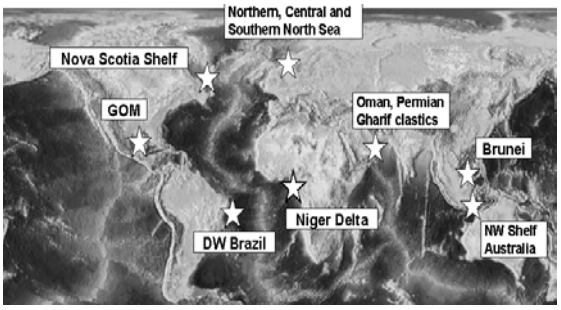

Figure 1. Map showing locations of field studies documenting multiple sand-on-sand sealing fault contacts. The occurrence of such sealing faults is independent of reservoir age and depositional environment (e.g., shallow or deep water), and generally independent of clay type, burial depth and history, and fault orientation with respect to regional stress.

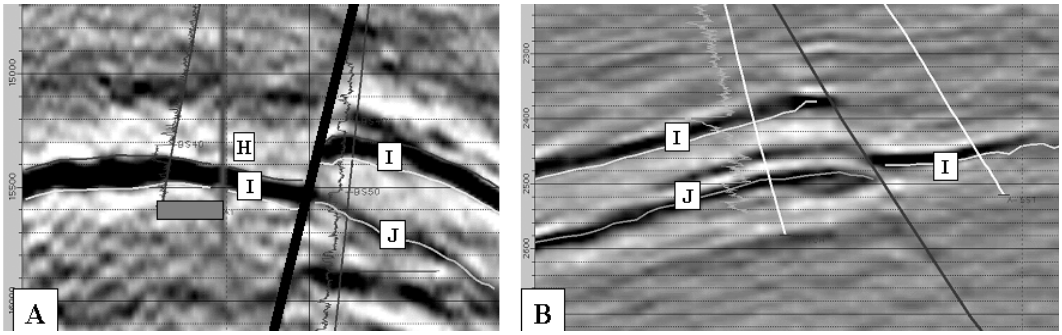

Figure 2. Examples of sealing sand-on-sand fault contacts in Tertiary deep-water reservoirs. (A) Downthrown gas-bearing I sand is in fault contact with upthrown wet J sand, requiring that the fault zone itself seal the two reservoirs. (B) Upthrown gas-bearing J sand is in fault contact with downthrown wet I sand, requiring that the fault zone seal. In both examples, the faults retain pressure differences of a few hundred psi prior to production, but retain pressure differences of thousands psi during field production.

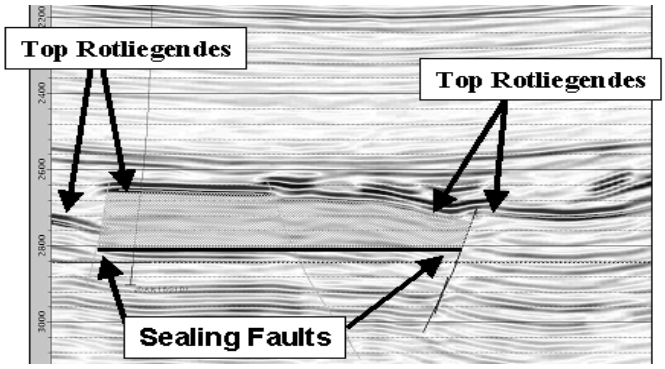

Figure 3. Examples of small-throw sealing faults where aeolian sandstones with ~100% net/gross are juxtaposed. The shaded area between the faults is a gas reservoir, while the same sandstones on the other sides of the faults are wet.

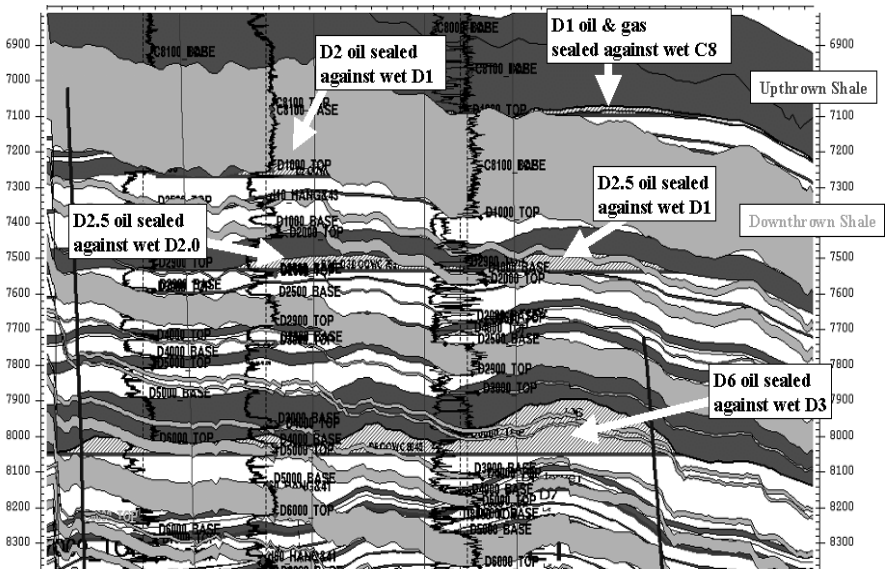

Figure 4. Example fault plane juxtaposition section showing multiple stacked pays that are trapped by sealing sand-on-sand fault contacts. This example is particularly illustrative because of the relatively thin shales, and the throw gradient along the fault. Because of these, possible or hypothetical variations in stratigraphy and/or throw

cannot eliminate the sealing sand-on-sand contacts.

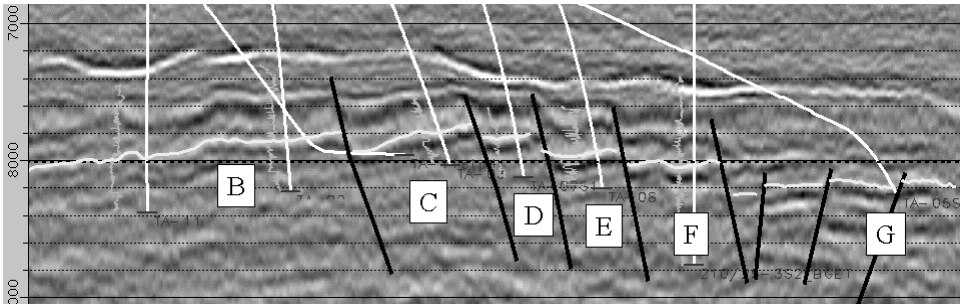

Figure 5. Example of sand-on-sand sealing fault contacts from a Brent field in the Northern North Sea. All faults juxtapose Jurassic Brent reservoir with Brent reservoir. The large-throw fault between blocks F and G is a hydraulic seal, retaining a 100 ft difference in the original oil-water contact, plus a 500 psi difference in the Brent aquifer gradients. The faults between B and C and C and D had no original cross-fault pressure difference, but retained on the order of 1000 psi production-induced pressure difference.

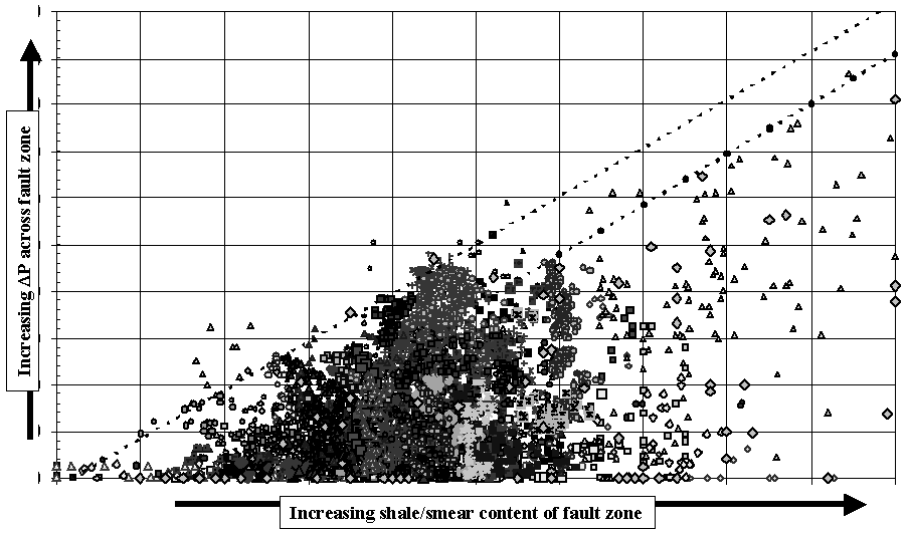

Figure 6. Cross plot of actual in situ fluid pressure differences as a function of fault zone composition. Data shown are from over one hundred fault-reservoir pairs from multiple basins as shown in Figure 1. The top of the data cloud increases linearly (and not logarithmically) as a function of the X values, indicating that higher X values retain greater fluid pressures. Note that there are fewer leaking fault occurrences (ΔP = 0 values) with increasing X, indicating that as X increases, the percentage of sealing faults also increases.

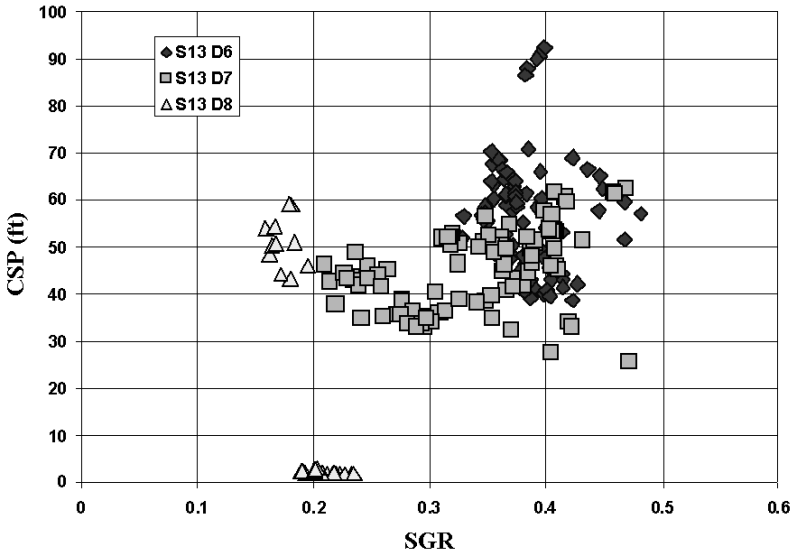

Figure 7. Cross plot of CSP as a function of SGR from points on 3 different reservoir-fault-reservoir contacts. There is no simple or direct correlation of CSP with SGR (or vice versa), consistent with the concept that they describe two significantly different physical processes.